Composite Structures 184 (2018) 1137–1144

Contents lists available at ScienceDirect

Composite Structures

journal homepage: www.elsevier.com/locate/compstruct

Nonlinear dynamic response and vibration of nanocomposite multilayer organic solar cell

Nguyen Dinh Duc[a,b,c,*], Kim Seung-Eock[c], Tran Quoc Quan[a,*], Dang Dinh Long[a], Vu Minh Anh[a,b]

[a] Advanced Materials and Structures Laboratory, VNU-Hanoi, University of Engineering and Technology, 144, Xuan Thuy, Cau Giay, Hanoi, Viet Nam
[b] Infrastructure Engineering Program, VNU-Hanoi, Vietnam-Japan University (VJU), My Dinh 1, Tu Liem, Hanoi, Viet Nam
[c] National Research Laboratory, Department of Civil and Environmental Engineering, Sejong University, 209 Neungdong-ro, Gwangjin-gu, Seoul 05006, Republic of Korea

ARTICLE INFO

Keywords:
Nanocomposite
Organic solar cell
Nonlinear dynamic and vibration
The classical plate theory
Imperfection

ABSTRACT

In the recent years, organic solar cell (OSC) has attracted much interest of the research community due to its great promise as renewable sources. This paper presents the first analytical approach to investigate the nonlinear dynamic response and vibration of imperfect rectangular nanocompsite multilayer organic solar cell subjected to mechanical loads using the classical plate theory. Nanocompsite organic solar cell consists of five layers of Al, P3HT:PCBM, PEDOT:PSS, IOT and glass. Motion and compatibility equations are derived using the classical plate theory and taking into account the effects of initial geometrical imperfection and geometrical nonlinearity in Von Karman – Donnell sense. The Galerkin method and fourth – order Runge – Kutta method are used to give explicit expressions of natural frequencies, nonlinear frequency – amplitude relation and nonlinear dynamic responses of nanocompsite organic solar cell. The numerical results show the influences of geometrical parameters, the thickness of layers, imperfections, and mechanical loads on the nonlinear dynamic response and nonlinear vibration of nanocompsite organic solar cell.

1. Introduction

Nanocomposite is a multiphase solid material where one of the phases has one, two or three dimensions of less than 100 nm (nm). Recently, nanocomposites are used in a number of fields and new applications such as automobiles, aerospace, injection molded products, coatings, adhesives, fire-retardants, packaging materials, microelectronic packaging, etc. Nanacomposites are usually added nanoparticles and fibers to enhance mechanical strength, toughness and electrical or thermal conductivity. The mechanical behaviors of nanocomposite with reinforced particles and fibers, such as bending, buckling, vibration, etc., have attracted attention of many researchers around the world. He et al. [1] investigated the mechanical behavior of hierarchical Mg matrix nanocomposite with high volume fraction reinforcement. Al-Lafi et al. [2] studied the mechanical responses of polycarbonate and polycarbonate/multi-walled carbon nanotubes to dynamic loadings at low and high velocities impacts were investigated experimentally using an instrumented falling weight impact tester and a split Hopkinson pressure bar, respectively. Asadi and Wang [3,4] investigated the aeroelastic analysis and dynamic stability analysis of functionally graded carbon nanotube reinforced composite beams and cylindrical shells subjected to aerodynamic load, axial compression and supersonic airflow. In 2015, Duc et al. [5] presented an investigation on the nonlinear dynamic response and vibration of the imperfect laminated three-phase polymer nanocomposite panel resting on elastic foundations and subjected to hydrodynamic loads. Souri et al. [6] introduced a theoretical study on the piezoresistive response of carbon nanotubes embedded in polymer nanocomposites in an elastic region; and Wu et al. [7] focused on the dynamic instability of functionally graded multilayer nanocomposite beams reinforced with a low content of graphene nanoplatelets and subjected to a combined action of a periodic axial force and a temperature change. Asadi et al. [8] considered the aero thermoelastic behaviors of supersonic functionally graded carbon nanotube reinforced composite flat panels in thermal environments. Further, Wang et al. [9] reported an improved in situ synthesis of PEDOT:PSS@AgNPs hybrid through simultaneous oxidation-reduction reaction between AgNO3 and EDOT at room temperature to achieve a hierarchical structure with excellent performance. Using a finite element-based multi-scale modeling approach, Ahmadi et al. [10] analyzed the bending, buckling and free vibration of hybrid polymer matrix composites reinforced by carbon fibers and carbon nanotubes. Mehri et al. [11] scrutinized the aeroelastic responses of functionally

* Corresponding authors at: Advanced Materials and Structures Laboratory, VNU-Hanoi, University of Engineering and Technology, 144, Xuan Thuy, Cau Giay, Hanoi, Viet Nam (Nguyen Dinh Duc, Tran Quoc Quan).
E-mail addresses: ducnd@vnu.edu.vn (N.D. Duc), quantq@vnu.edu.vn (T.Q. Quan).

http://dx.doi.org/10.1016/j.compstruct.2017.10.064
Received 26 July 2017; Received in revised form 17 October 2017; Accepted 21 October 2017
Available online 21 October 2017
0263-8223/

graded carbon nanotube reinforced composite truncated conical curved panels subjected to aerodynamic load and axial compression. Based on the classical plate theory, Duc and Thu [12] presented an analytical approach to investigate the non-linear dynamic response and vibration of an imperfect three-phase laminated nanocomposite plate and cylindrical panel resting on elastic foundations in thermal environments. Wu et al. [13] dealt with the thermal buckling and postbuckling of functionally graded multilayer nanocomposite plates reinforced with a low content of graphene platelets.

Organic solar cell (OSC) is well-known as a renewable energy device owning the light and flexible properties which could be expected as the next generation of the solar cell technology [14–16]. Multilayer composite structure is the key factor for these photovoltaic devices such as nanocomposite composed of multilayer structure with nanoparticles embedded in polymers (NIP) and polymers deposited on nanoporous thin films (PON) for OSC [17]. Interestingly, several nanostructures such as nanoparticle and nanorodsare believed to improve the light harvesting process through the localized surface plasmon resonance (LSPR) effect [18–21]. In this work, we have embedded nanocrystalline such as TiO_2or ZnO inside PEDOT-PSS as well as P3HT:PCBM [22]. On one hand, the higher quenching of the polymer fluorescence observed in presence of TiO_2 nanoparticles indicates that the transfer of the photogenerated electrons to the TiO_2 is more efficient than rods. On the other hand, the absorption spectrum in the visible light induced by nanorods has been increased about 20% more than nanoparticles. Characterization of the nanocomposite films showed that both the current-voltage characteristics and the photoluminescent properties of the nanocomposite materials were significantly enhanced in comparison with the pure polymers. The role of the buffer layer, i.e. ZnO thin film, in OSC structure will also be discussed in this work. The optimal thickness layer of OSC will be simulated by the diode model fitting to JV characteristics. In order to investigate the operating-temperature range for photovoltaic device parameters, a P3HT + nc-TiO_2 composite photoactive layer was prepared. The photovoltaic conversion efficiency was reached a value of 1.72%. The enhancement in the photoelectrical conversion efficiency of the solar composite-based cells is attributed to the presence of nano-hetero junctions of TiO_2/P3HT and ZnO/P3HT:PCBM. For the temperature range of (30–70) °C, the decrease of the open-circuit potential was compensated by an increase of the fill factor; and the increase in the short-circuit current resulted in an overall increase of the energy conversion efficiency. At elevated temperatures of 60–80 °C the efficiency of the pure P3HT-OSC reached a maximum value of 1.6% and 2.1%, respectively. Over this temperature range the efficiency of P3HT-based cell decreased strongly to zero, while for the composite cells it maintained a value as large as 1.2% at a temperature range of (110–140) °C. The static and dynamic stability of OSC under different loads such as the thermal load and mechanical load have been investigated using the classical shear theory [23]. In general, we have shown that the combination of rods and nanoparticles in the nanocomposite material is able to stabilize the composite structures. Recently, the reinforce of polymers using more complex structure such as auxetic layer and piezoelectric layer, nanoparticles not only increases the strength of the material but also enriches the physical properties of nanocomposite structure. The applications of piezoelectric layers and carbon nanotubes in enhancing nonlinear vibration behaviors and suppressing the postbuckling deflection of functionally graded carbon nanotube reinforced composite annular plates is presented [24,25]. For an illustration purpose, the Young's module, Poisson's ratio, bulk module and other elastic modulus of composite materials will also be discussed [26–28].

This paper presents the first analytical approach to investigate the nonlinear dynamic response and vibration of the imperfect nanocompsite multilayer organic solar cell subjected to mechanical loads. By using the Galerkin method and fourth – order Runge – Kutta method, the influences of geometrical parameters, the thickness of layers, imperfections, mechanical loads on the nonlinear dynamic response and nonlinear vibration of solar cells are discussed in details.

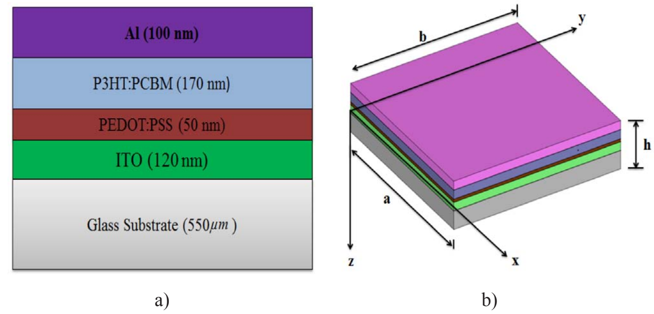

Fig. 1. Geometry and coordinate system of nanocompsite multilayer organic solar cell. (a) 2D model (b) 3D model.

2. The modelling of nanocompsite multilayer organic solar cell

Consider a rectangular nanocompsite organic solar cell with five layers of length of edges a, b and total thickness h as shown in Fig. 1. Five layers are made of Al, P3HT:PCBM, PEDOT:PSS, IOT and glass, respectively. Each layer is assumed to be isotropic and the thickness, Young modulus and Poisson's ratio of each layer are h_k, E_k. and ν_k, $(k = \overline{1,5})$ respectively. A coordinate system (x,y,z) is established in which (x,y) plane on the middle surface of the cell and z on thickness direction $(-h/2 \leqslant z \leqslant h/2)$ as shown in Fig. 1.

3. Basic equations

In this study, the classical plate theory is used to derive basic equations to investigate the nonlinear dynamic response and vibration of nanocompsite multilayer organic solar cell.

The strain – displacement relation taking into account the Von Karman non – linear terms are [31–33]

$$\begin{pmatrix} \varepsilon_x \\ \varepsilon_y \\ \gamma_{xy} \end{pmatrix} = \begin{pmatrix} \varepsilon_x^0 \\ \varepsilon_y^0 \\ \gamma_{xy}^0 \end{pmatrix} + z \begin{pmatrix} k_x^1 \\ k_y^1 \\ k_{xy}^1 \end{pmatrix} \tag{1}$$

where

$$\begin{pmatrix} \varepsilon_x^0 \\ \varepsilon_y^0 \\ \gamma_{xy}^0 \end{pmatrix} = \begin{pmatrix} \frac{\partial u}{\partial x} + \frac{1}{2}\left(\frac{\partial w}{\partial x}\right)^2 \\ \frac{\partial v}{\partial y} + \frac{1}{2}\left(\frac{\partial w}{\partial y}\right)^2 \\ \frac{\partial u}{\partial y} + \frac{\partial v}{\partial x} + \frac{\partial w}{\partial x}\frac{\partial w}{\partial y} \end{pmatrix}, \quad \begin{pmatrix} k_x \\ k_y \\ k_{xy} \end{pmatrix} = \begin{pmatrix} -w_{,xx} \\ -w_{,yy} \\ -2w_{,xy} \end{pmatrix}, \tag{2}$$

in which u,v are the displacement components along the x,y directions, respectively.

The stress–strain relationships for the nanocompsite multilayer organic solar cell are defined by the Hooke's law as

$$\begin{pmatrix} \sigma_x \\ \sigma_y \\ \sigma_{xy} \end{pmatrix}_k = \begin{pmatrix} Q'_{11} & Q'_{12} & Q'_{16} \\ Q'_{12} & Q'_{22} & Q'_{26} \\ Q'_{16} & Q'_{26} & Q'_{66} \end{pmatrix}_k \begin{pmatrix} \varepsilon_x \\ \varepsilon_y \\ \gamma_{xy} \end{pmatrix}_k, \tag{3}$$

with k is the number of layers of nanocompsite organic solar cell and

$$Q'_{11k} = \frac{E_k}{1-\nu_k^2}, Q'_{12k} = \frac{\nu_k E_k}{1-\nu_k^2}, Q'_{16k} = 0, Q'_{22k} = \frac{E}{1-\nu_k^2}, Q'_{26k} = 0, Q'_{66k} = \frac{E_k}{2(1+\nu_k)}. \tag{4}$$

The force and moment resultants of nanocompsite multilayer organic solar cell are given by

$$N_i = \sum_{k=1}^{n} \int_{h_{k-1}}^{h_k} [\sigma_i]_k dz, i = x,y,xy, M_i = \sum_{k=1}^{n} \int_{h_{k-1}}^{h_k} z[\sigma_i]_k dz, i = x,y,xy. \quad (5)$$

Substitution of Eq. (1) into Eq. (3) and the results into Eq. (5) give the constitutive relations as

$$\begin{bmatrix} N_x \\ N_y \\ N_{xy} \\ M_x \\ M_y \\ M_{xy} \end{bmatrix} = \begin{bmatrix} A_{11} & A_{12} & 0 & B_{11} & B_{12} & 0 \\ A_{12} & A_{22} & 0 & B_{12} & B_{22} & 0 \\ 0 & 0 & A_{66} & 0 & 0 & B_{66} \\ B_{11} & B_{12} & 0 & D_{11} & D_{12} & 0 \\ B_{12} & B_{22} & 0 & D_{12} & D_{22} & 0 \\ 0 & 0 & B_{66} & 0 & 0 & D_{66} \end{bmatrix} \begin{bmatrix} \varepsilon_x^0 \\ \varepsilon_y^0 \\ \gamma_{xy}^0 \\ k_x \\ k_y \\ k_{xy} \end{bmatrix}, \quad (6)$$

where the detail of coefficients $X_{11}, X_{12}, X_{22}, X_{66}$ $(X = A, B, D)$ may be found in Appendix A.

The nonlinear equilibrium equations of a nanocompsite multilayer organic solar cell based on the classical plate theory are [31–33]

$$N_{x,x} + N_{xy,y} = 0, N_{xy,x} + N_{y,y} = 0, M_{x,xx} + 2M_{xy,xy} + M_{y,yy} + N_x w_{,xx} + 2N_{xy} w_{,xy} + N_y w_{,yy} + q = \rho_1 \frac{\partial^2 w}{\partial t^2}, \quad (7)$$

in which the material damping is not taken into account because of its small influence.

The geometrical compatibility equation for an imperfect nanocompsite multilayer organic solar cell is written as [31–33]

$$\varepsilon_{x,yy}^0 + \varepsilon_{y,xx}^0 - \gamma_{xy,xy}^0 = w_{,xy}^2 - w_{,xx} w_{,yy} + 2w_{,xy} w_{,xy}^* - w_{,xx} w_{,yy}^* - w_{,yy} w_{,xx}^*. \quad (8)$$

$f(x,y)$ is stress function defined by [5,12]

$$N_x = \frac{\partial^2 f}{\partial y^2}, N_y = \frac{\partial^2 f}{\partial x^2}, N_{xy} = -\frac{\partial^2 f}{\partial x \partial y}. \quad (9)$$

From the constitutive relation (6), one can write

$$\varepsilon_x^0 = A_{11}^* N_x + A_{12}^* N_y + A_{13}^* k_x + A_{14}^* k_y, \varepsilon_y^0 = A_{22}^* N_y + A_{12}^* N_x + A_{23}^* k_x + A_{24}^* k_y, \gamma_{xy}^0 = A_{31}^* N_{xy} + A_{32}^* k_{xy}, \quad (10)$$

with the detail of coefficients $A_{1i}^* (i = \overline{1,4})$, $A_{2j}^* (j = \overline{2,4})$, $A_{3k}^* (k = 1,2)$ are given in Appendix A.

By substituting Eq. (10) into Eq. (6) and then into Eq. (7) with the aid of Eq. (8), the system of motion Eq. (7) is rewritten as follows

$$T_{11} f_{,xxxx} + T_{12} f_{,yyyy} + T_{13} f_{,xyxy} + T_{14} w_{,xxxx} + T_{15} w_{,yyyy} + T_{16} w_{,xyxy} + f_{,yy} w_{,xx} - 2f_{,xy} w_{,xy} + f_{,xx} w_{,yy} + q = \rho_1 \frac{\partial^2 w}{\partial t^2}. \quad (11)$$

where the linear operators $T_{1j} (j = \overline{1,6})$ are given Appendix A.

For an imperfect nanocompsite multilayer organic solar cell, Eq. (11) is modified into form as

$$T_{11} f_{,xxxx} + T_{12} f_{,yyyy} + T_{13} f_{,xyxy} + T_{14}(w_{,xxxx} + w_{,xxxx}^*) + T_{15}(w_{,yyyy} + w_{,yyyy}^*) + T_{16}(w_{,xyxy} + w_{,xyxy}^*) + f_{,yy}(w_{,xx} + w_{,xx}^*) - 2f_{,xy}(w_{,xy} + w_{,xy}^*) + f_{,xx}(w_{,yy} + w_{,yy}^*) + q = \rho_1 \frac{\partial^2 w}{\partial t^2}. \quad (12)$$

From Eq. (10) in conjunction with Eq. (9) we have

$$\varepsilon_x^0 = A_{11}^* f_{,yy} + A_{12}^* f_{,xx} - A_{13}^* w_{,xx} - A_{14}^* w_{,yy},\ \varepsilon_y^0 = A_{22}^* f_{,xx} + A_{12}^* f_{,yy} - A_{23}^* w_{,xx} - A_{24}^* w_{,yy},\ \gamma_{xy}^0 = -A_{31}^* f_{,xy} - 2A_{32}^* w_{,xy}. \quad (13)$$

Setting Eq. (13) into Eq. (8) gives the compatibility equation of an imperfect nanocompsite multilayer organic solar cell as

$$A_{11}^* f_{,yyyy} + A_{12}^* f_{,xxyy} - A_{13}^* w_{,xxyy} - A_{14}^* w_{,yyyy}, A_{22}^* f_{,xxxx} + A_{12}^* f_{,xxyy} - A_{23}^* w_{,xxxx} - A_{24}^* w_{,yyxx}, + A_{31}^* f_{,xxyy} + 2A_{32}^* w_{,xxyy} = w_{,xy}^2 - w_{,xx} w_{,yy} + 2w_{,xy} w_{,xy}^* - w_{,xx} w_{,yy}^* - w_{,yy} w_{,xx}^*. \quad (14)$$

Eqs. (12) and (14) are nonlinear equations in term of variables w and f and used to investigate the nonlinear dynamic response and vibration of imperfect nanocompsite multilayer organic solar cell under mechanical loads using the classical plate theory.

4. Nonlinear vibration analysis

Assume an imperfect nanocompsite multilayer organic solar cell with freely movable edges is subjected to uniformly distributed pressure of intensity q. Thus the boundary conditions are

$$w = N_{xy} = M_x = P_x = 0, N_x = N_{x0} at x = 0,a w = N_{xy} = M_y = P_y = 0, N_y = N_{y0} at y = 0,b \quad (15)$$

where N_{x0}, N_{y0} are in-plane compressive loads at movable edges.

The approximate solutions of w and f satisfying boundary conditions (15) are assumed to be [5,12,29,30,33]

$$w = W\sin\alpha x\sin\beta y, f = A_1\cos 2\alpha x + A_2\cos 2\beta y + A_3\sin\alpha x\sin\beta y + \frac{1}{2}N_{x0}y^2 + \frac{1}{2}N_{y0}x^2, \quad (16)$$

where $\alpha = m\pi/a$, $\beta = n\pi/b$, m,n are odd natural numbers representing the number of half waves in the x and y directions, respectively; and $W(t)$ are the time dependent amplitudes.

The initial imperfection w^* is assumed to have the same form of the organic solar cell deflection w, i.e. [5,12,29,30,33]

$$w^*(x,y) = W_0\sin\alpha x\sin\beta y, \quad (17)$$

in which W_0 is imperfection amplitude of the nanocompsite multilayer organic solar cell.

Introducing Eqs. (16) and (17) into the compatibility equation (14) and solving obtained equation for unknown f leads to

$$A_2 = \frac{(W^2 + 2WW_0)\alpha^2}{32A_{11}^*\beta^2},\ A_1 = \frac{(W^2 + 2WW_0)\beta^2}{32A_{22}^*\alpha^2},\ A_3 = \frac{A_{14}^*\beta^4 + A_{23}^*\alpha^4 - (2A_{32}^* - A_{13}^* - A_{24}^*)\alpha^2\beta^2}{A_{11}^*\beta^4 + A_{22}^*\alpha^4 + (A_{12}^* + A_{12}^* + A_{31}^*)\alpha^2\beta^2} W. \quad (18)$$

Replacing Eqs. (16)–(18) into Eqs. (12) and then applying Galerkin method to the resulting equations yields

$$S_1(W + 2W_0)W + S_2W + S_3(W^2 + 2WW_0)(W + W_0) - (\alpha^2 N_x^0 + \beta^2 N_y^0)(W + W_0) + S_4(W + W_0)W + S_5(W + W_0) + S_6 q = \rho_1 \frac{\partial^2 w}{\partial t^2}. \quad (19)$$

where the detail of coefficients $S_i (i = \overline{1,6})$ are given in Appendix A.

This is basic equation to determine nonlinear dynamic response of a nanocompsite multilayer organic solar cell subjected to mechanical loads.

4.1. Nonlinear dynamic response

Consider a nanocompsite multilayer organic solar cell with freely movable edges only subjected to uniform external pressure $q = Q\sin\Omega t$ (Q is the amplitude of uniformly excited load, Ω is the frequency of the load) and uniform compressive forces P_x and P_y (Pascal) on the edges $x = 0,a$ và $y = 0,b$. In this case, $N_x^0 = -P_x h$, $N_y^0 = -P_y h$ and Eq. (19) is reduced to

$$S_1(W + 2W_0)W + S_2W + S_3(W^2 + 2WW_0)(W + W_0) + (\alpha^2 P_x - \beta^2 P_y)h(W + W_0) + S_4(W + W_0)W + S_5(W + W_0) + S_6 Q\sin\Omega t = \rho_1 \frac{\partial^2 w}{\partial t^2}. \quad (20)$$

By using Eq. (20), three aspects are taken into consideration: fundamental frequencies of natural vibration of the nanocompsite multilayer organic solar cell, frequency – amplitude relation of nonlinear free vibration and nonlinear dynamic response of nanocompsite multilayer organic solar cell. The nonlinear dynamic responses of the nanocompsite multilayer organic solar cell can be obtained by solving this equation combined with initial conditions to be assumed as $W(0) = 0, \frac{dW}{dt}(0) = 0$ by using the fourth – order Runge – Kutta method.

4.2. Natural frequency and amplitude – Frequency relation

The fundamental frequencies of a perfect organic solar cell can be determined approximately by an explicit expression from Eq. (20) as

$$\omega_{mn} = \sqrt{-\frac{S_2 + S_5 + (\alpha^2 P_x + \beta^2 P_y)h}{\rho_1}}. \tag{21}$$

Consider nonlinear vibration of a perfect organic solar cell, Eq. (20) has of the form

$$\frac{\partial^2 W}{\partial t^2} + \omega_{mn}(W + MW^2 + NW^3) - F\sin(\Omega t) = 0, \tag{22}$$

where

$$M = \frac{S_1 + S_4}{S_2 + S_5 + (\alpha_m^2 P_x + \beta_n^2 P_y)h}, N = \frac{S_3}{S_2 + S_5 + (\alpha_m^2 P_x + \beta_n^2 P_y)h}, F = \frac{S_6}{\rho_1}Q. \tag{23}$$

Seeking solution as $W = A\sin\Omega t$ and applying Galerkin procedure to Eq. (22), the amplitude – frequency relation of nonlinear forced vibration is obtained as

$$\chi^2 - \left(1 - \frac{8}{3\pi}MA + \frac{3}{4}NA^2\right) + \frac{F}{A\omega_{mn}^2} = 0. \tag{24}$$

where

$$\chi = \Omega/\omega_{mn} \tag{25}$$

If $F = 0$, i.e. no excitation acting on the organic solar cell, the frequency –amplitude relation of the free nonlinear vibration is obtained as

$$\omega_{NL}^2 = \omega_{mn}^2\left(1 - \frac{8}{3\pi}MA + \frac{3}{4}NA^2\right). \tag{26}$$

5. Results and discussion

This section presents the illustrative results for nanocompsite multilayer organic solar cell with the thickness and the material properties of each layer given as in Table 1.

5.1. Natural frequency

The effects of thickness of layers $h_{Al}, h_{PCBM}, h_{PSS}, h_{ITO}$ and modes (m,n) on the natural oscillation frequency of the nanocompsite multilayer organic solar cell are shown in Table 2. It is easy to see that the value of the natural oscillation frequency increases when the thickness of layers increase and the value of modes increase. The Table 2 also shows that the effect of ITO layer on natural oscillation frequency of the nanocompsite multilayer organic solar cell is highest and the effect of PSS layer on natural oscillation frequency of the nanocompsite multilayer organic solar cell is lowest in five layers. This conclusion is easy to explain because the elastic modulus of ITO layer is highest and the elastic modulus of PSS layer is lowest of all. The Table 2 also shows that the natural oscillation frequency increases when modes (m,n) increase.

Table 1
The thickness and material properties of the constituent materials of the considered nanocompsite multilayer organic solar cell.

Layers	Thickness	E (GPa)	ν	ρ (kg/m^3)
Al	100 nm	70	0.35	2601
P3HT:PCBM	170 nm	6	0.23	1200
PEDOT:PSS	50 nm	2.3	0.4	1000
ITO	120 nm	116	0.35	7120
Glass Substrate	550 µm	69	0.23	2400

5.2. Dynamic response

5.2.1. Effect of geometrical parameter

Fig. 2 illustrates the effect of geometric factor a/b on nonlinear dynamic response of nanocompsite multilayer organic solar cell with $P_x = 0, P_y = 0$. From Fig. 2, the deflection amplitude of the organic solar cell increases when increasing the ratio a/b. In a fabricating process, the ratio a/b has been chosen as close as a square shape cell. In other words, the best ratio a/b for an experiment is 1.0 [34], hence our finding is consistent with the experiments. This result has reconfirmed the best shape for the organic solar cell sample is a square instead of a rectangular.

5.2.2. Effect of the thickness of layers

Figs. 3–5 indicate the effect of the thickness of PCBM layer, PSS layer and ITO layer on the nonlinear dynamic response of the nanocompsite multilayer organic solar cell with $a = b = 1$, $P_x = 0, P_y = 0$, respectively. It can be seen that the deflection amplitude of the nonlinear dynamic response of the solar cell decreases when the thickness of these layers increases. Because of the trade-off between the recombination of the electron-hole pairs and the collection of the exciton in organic solar cell, the optimal thickness of the active layer is limited to approximately 200 nm [18].

Hence, our finding is important since the dynamic response of the solar cell does not depend strongly on the thickness of each layer. In other words, we do not need to be worried about stability of the solar cell within a range of the thickness order from 170 to700 nm for PCBM, from 50 to 900 nm for PSS, from 50 to 135 nm for ITO.

5.2.3. Effect of mechanical loads

Fig. 6 considers the effect of harmonic uniform exciting force with amplitudes $Q = 100$ N/m^2 [$Q = 250$ N/m^2 and $Q = 300$ N/m^2 on the dynamic response of nanocompsite multilayer organic solar cell. From these figures, it is seen that the nonlinear deflection amplitude of the organic solar cell is considerably increased when excitation force amplitude Q increases.

Figs. 7 and 8 show nonlinear dynamic response of the nanocompsite multilayer organic solar cell with various values of the pre-loaded axial compression P_x, P_y. Clearly, the higher value of the pre-loaded axial compression is, the higher nonlinear deflection amplitude of the organic solar cell is.

5.2.4. Effect of imperfection

The effect of initial imperfection W_0 on the dynamic response of nanocompsite multilayer organic solar cell is indicated in Fig. 9. As expected, the reduction of amplitude of initial imperfection makes the deflection amplitude of nonlinear vibration of the organic solar cell decrease.

5.3. Frequency – Amplitude relation

5.3.1. Effect of external force F

Fig. 10 shows the effect of external force F on the frequency – amplitude relations of frequency – amplitude curves of the nanocompsite multilayer organic solar cell. As can be seen, when the excitation force decreases, the curves of forced vibration are closer to the curve of free vibration.

Table 2
Effects of the thickness of layers and modes on natural frequencies of the nanocompsite multilayer organic solar cell.

h_{Al} (nm)	h_{PCBM} (nm)	h_{PSS} (nm)	h_{ITO} (nm)	(m,n)			
				(1,1)	(1,3)	(3,3)	(3,5)
100	170	50	120	19011	71192	171100	286770
120	170	50	120	19733	72940	177600	297540
100	185	50	120	19040	71261	171360	287200
100	170	65	120	19032	71243	171290	287090
100	170	50	135	19808	73121	178270	298660
120	185	65	135	20548	74938	184940	309710
135	195	70	160	22265	79231	200390	335350
150	210	90	170	23227	81679	209050	349720

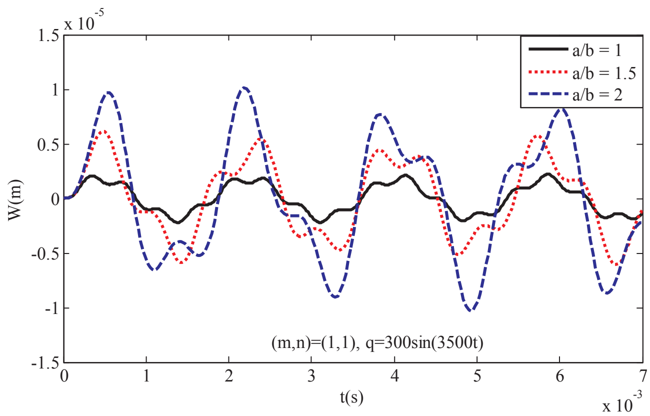

Fig. 2. Effect of ratio a/b on the nonlinear dynamic response of nanocompsite multilayer organic solar cell ($P_x = 0, P_y = 0$).

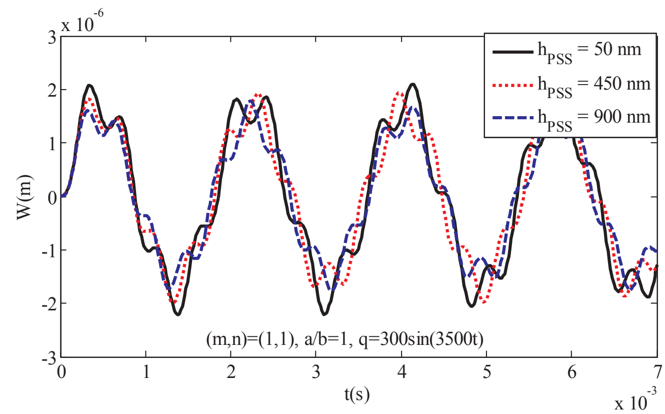

Fig. 4. Effect of the thickness of PSS layer on the dynamic response of nanocompsite multilayer organic solar cell ($P_x = 0, P_y = 0$).

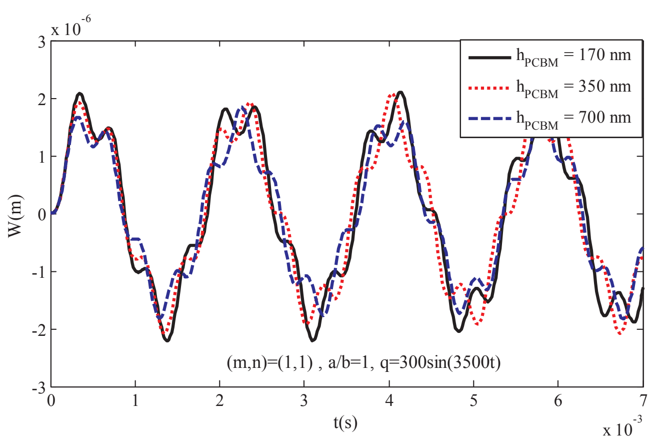

Fig. 3. Effect of the thickness of PCBM layer on the dynamic response of nanocompsite multilayer organic solar cell ($P_x = 0, P_y = 0$).

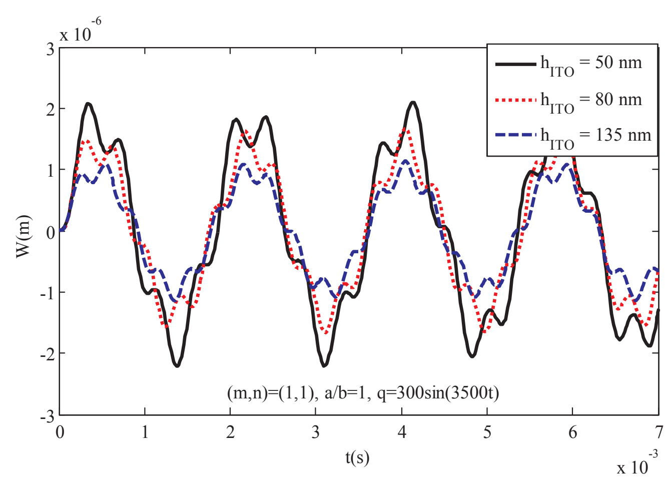

Fig. 5. Effect of the thickness of ITO layer on the dynamic response of nanocompsite multilayer organic solar cell ($P_x = 0, P_y = 0$).

5.3.2. Effect of the thickness of layers

Fig. 11 shows the effects of the thickness of ITO layer on the frequency – amplitude relations of the nanocompsite multilayer organic solar cell. One can see that with the same dynamic amplitude, nanocompsite multilayer organic solar cell with lower thickness have smaller frequency than the nanocompsite multilayer organic solar cell with higher thickness.

6. Conclusions

This paper investigated the nonlinear dynamic response and vibration of the nanocompsite multilayer organic solar cell subjected to mechanical loads based on the classic plate theory taking into account geometrical nonlinearity and initial geometrical imperfection. By using Galerkin method and fourth – order Runge – Kutta method, the influence of the geometrical parameter, the thickness of layers, initial imperfection and mechanical loads on the nonlinear dynamic response and vibration of the solar cell are examined in detail. Some conclusions can be obtained from the present analysis:

- The thickness of every layer of organic solar cell has a significant influence on the nonlinear dynamic response and nonlinear vibration of the nanocompsite multilayer organic solar cell.
- The effect of ITO layer on nonlinear vibration of the nanocompsite multilayer organic solar cell is highest and the effect of PSS layer on nonlinear vibration of the nanocompsite multilayer organic solar cell is lowest in five layers.

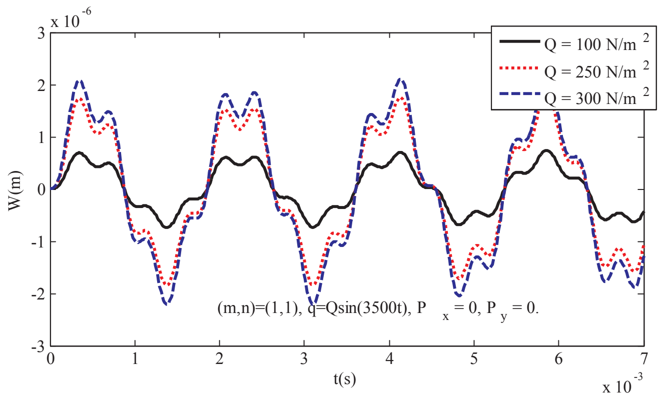

Fig. 6. Effect of the exciting force amplitude Q on the dynamic response of nanocompsite multilayer organic solar cell ($P_x = 0, P_y = 0$).

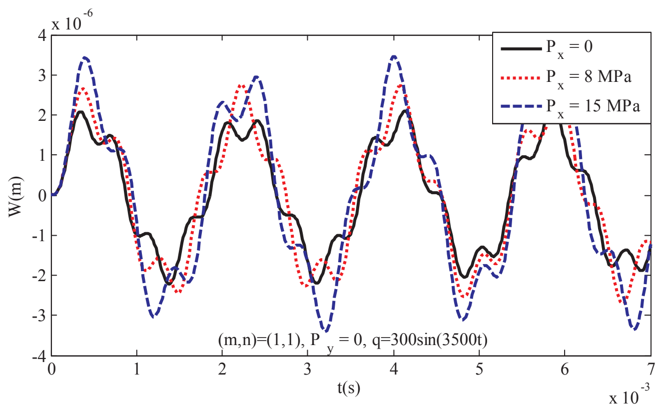

Fig. 7. Effect of the pre-loaded axial compression P_x on the dynamic response of nanocompsite multilayer organic solar cell.

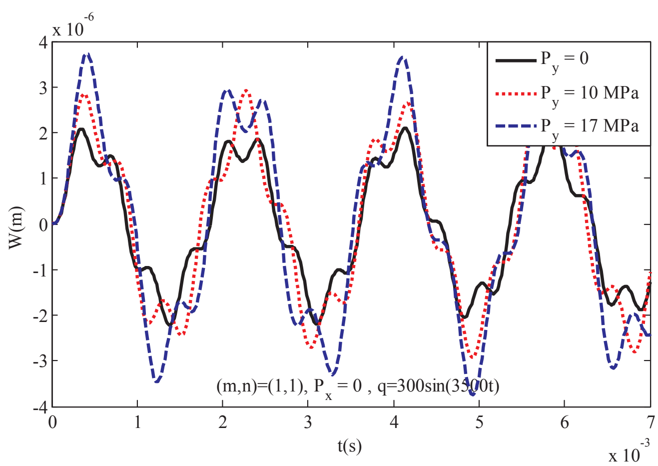

Fig. 8. Effect of the pre-loaded axial compression P_y on the dynamic response of nanocompsite multilayer organic solar cell.

– The nonlinear dynamic amplitude of the nanocompsite solar cell is considerably increased when excitation force amplitude Q and P_x increase.
– Initial geometrical imperfection has negative influence on the nonlinear dynamic response and vibration of nanocompsite multilayer organic solar cell.

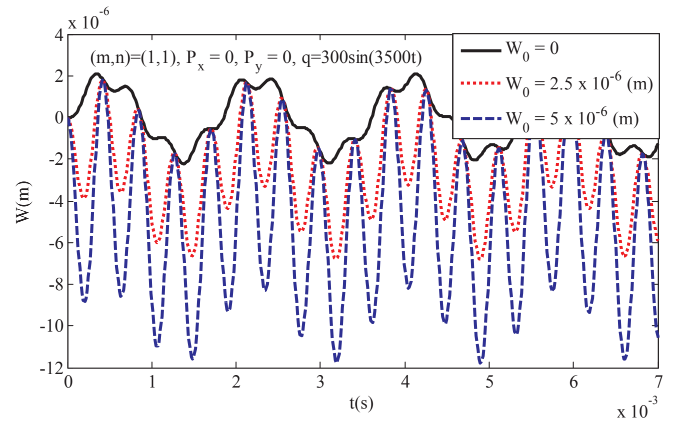

Fig. 9. Effect of initial imperfection W_0 on the dynamic response of nanocompsite multilayer organic solar cell.

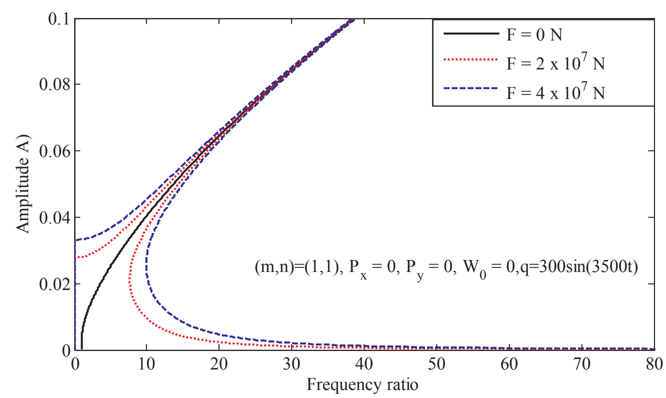

Fig. 10. Effect of external force F on frequency – amplitude curves of the nanocompsite multilayer organic solar cell.

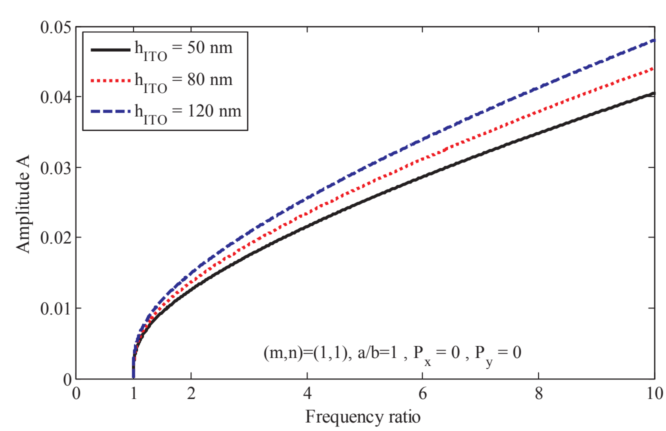

Fig. 11. Effect of the thickness of ITO layer on frequency – amplitude curves of the nanocompsite multilayer organic solar cell.

Acknowledgement

This work was supported by the Vietnam National University, Hanoi. The authors are grateful for this support.

Appendix A

$$A_{11} = \sum_{k=1}^{5} \frac{E_k h_k}{1-v_k^2},\ A_{12} = \sum_{k=1}^{5} \frac{v_k E_k h_k}{1-v_k^2}, A_{22} = A_{11},$$

$$A_{16} = A_{26} = 0, A_{66} = \sum_{k=1}^{5} \frac{E_k h_k}{2(1+v_k)},$$

$$B_{11} = \sum_{k=1}^{5} \frac{E_k h_k z_k}{1-v_k^2}, B_{12} = \sum_{k=1}^{5} \frac{v_k E_k h_k z_k}{1-v_k^2}; B_{22} = B_{11},$$

$$B_{16} = B_{26} = 0, B_{66} = \sum_{k=1}^{5} \frac{E_k h_k z_k}{2(1+v_k)},$$

$$D_{11} = \sum_{k=1}^{5} \frac{E_k}{1-v_k^2}\left(h_k z_k^2 + \frac{h_k^3}{12}\right), D_{12} = \sum_{k=1}^{5} \frac{v_k E_k h_k z_k}{1-v_k^2}, D_{22} = D_{11},$$

$$D_{16} = D_{26} = 0, D_{66} = \sum_{k=1}^{n} \frac{E_k}{2(1+v_k)}\left(h_k z_k^2 + \frac{h_k^3}{12}\right),$$

$$\Delta = A_{22}A_{11}-A_{12}^2, A_{31}^* = \frac{1}{A_{66}}, A_{32}^* = -\frac{B_{66}}{A_{66}},$$

$$A_{11}^* = \frac{A_{22}}{\Delta}, A_{12}^* = -\frac{A_{12}}{\Delta}, A_{13}^* = \frac{A_{12}B_{12}-A_{22}B_{11}}{\Delta}, A_{14}^* = \frac{A_{12}B_{22}-A_{22}B_{12}}{\Delta},$$

$$A_{22}^* = \frac{A_{11}}{\Delta}, A_{23}^* = \frac{A_{12}B_{11}-A_{11}B_{12}}{\Delta}, A_{24}^* = \frac{A_{12}B_{12}-A_{11}B_{22}}{\Delta},$$

$$T_{11} = (B_{11}A_{12}^* + B_{12}A_{22}^*), T_{12} = (B_{12}A_{11}^* + B_{22}A_{12}^*),$$

$$T_{13} = [(B_{11}A_{11}^* + B_{12}A_{12}^*) + (B_{12}A_{12}^* + B_{22}A_{22}^*)-2B_{66}A_{31}^*],$$

$$T_{14} = +(-B_{11}A_{13}^*-B_{12}A_{23}^*-D_{11}), T_{15} = +(-B_{12}A_{14}^*-B_{22}A_{24}^*-D_{22}),$$

$$T_{16} = +\begin{bmatrix} -B_{11}A_{14}^*-B_{12}A_{24}^*-D_{12}-B_{12}A_{13}^* \\ -B_{22}A_{23}^*-D_{12}-4B_{66}A_{32}^*-4D_{66} \end{bmatrix},$$

$$S_1 = \left(\frac{T_{11}}{A_{22}^*} + \frac{T_{12}}{A_{11}^*}\right)\left(\frac{-8\alpha\beta}{3ab}\right)(W+2W_0)W,$$

$$S_2 = +\left[(T_{11}\alpha^4 + T_{12}\beta^4 + T_{13}\alpha^2\beta^2)\frac{[A_{14}^*\beta_n^4 + A_{23}^*\alpha_m^4-(2A_{32}^*-A_{13}^*-A_{24}^*)\alpha_m^2\beta_n^2]}{[A_{11}^*\beta_n^4 + A_{22}^*\alpha_m^4 + (A_{12}^* + A_{12}^* + A_{31}^*)\alpha_m^2\beta_n^2]}\right]W,$$

$$S_3 = -\frac{\beta^4}{8A_{22}^*}(W^2 + 2WW_0)(W + W_0),$$

$$S_4 = \beta\alpha\frac{4}{ab}\left(\frac{32}{9}-\frac{8}{9}\right)\frac{A_{14}^*\beta^4 + A_{23}^*\alpha^4-(2A_{32}^*-A_{13}^*-A_{24}^*)\alpha^2\beta^2}{A_{11}^*\beta^4 + A_{22}^*\alpha^4 + (A_{12}^* + A_{12}^* + A_{31}^*)\alpha^2\beta^2}(W + W_0)W,$$

$$S_5 = (T_{14}\alpha^4 + T_{15}\beta^4 + T_{16}\alpha^2\beta^2)(W + W_0), S_6 = \frac{4}{ab}.$$

References

[1] He X, Liu J, An L. The mechanical behavior of hierarchical Mg matrix nanocomposite with high volume fraction reinforcement. Mater Sci Eng, A 2017;699:114–7.

[2] Al-Lafi W, Jin J, Song M. Mechanical response of polycarbonate nanocomposites to high velocity impact. Eur Polymer J 2016;85:354–62.

[3] Asadi H, Wang Q. An investigation on the aeroelastic flutter characteristics of FG-CNTRC beams in the supersonic flow. Compos B Eng 2017;116:486–99.

[4] Asadi H, Wang Q. Dynamic stability analysis of a pressurized FG-CNTRC cylindrical shell interacting with supersonic airflow. Compos B Eng 2017;118:15–25.

[5] Duc ND, Hadavinia H, Van ThuP, Quan TQ. Vibration and nonlinear dynamic response of imperfect three-phase polymer nanocomposite panel resting on elastic foundations under hydrodynamic loads. Compos Struct 2015;131:229–37.

[6] Souri H, Yu J, Jeon H, Woo J, Yang C, You N, et al. A theoretical study on the piezoresistive response of carbon nanotubes embedded in polymer nanocomposites in an elastic region. Carbon 2017;120:427–37.

[7] Wu H, Yang J, Kitipornchai S. Dynamic instability of functionally graded multilayer graphene nanocomposite beams in thermal environment. Compos Struct 2017;162:244–54.

[8] Asadi H, Souri M, Wang Q. A numerical study on flow-induced instabilities of supersonic FG-CNT reinforced composite flat panels in thermal environments. Compos Struct 2017;171:113–25.

[9] Wang Y, Pang FF, Liu DD, Han GZ. In situ synthesis of PEDOT:PSS@AgNPs nanocomposites. Synth Met 2017;230:1–6.

[10] Ahmadi M, Ansari R, Rouhi H. Multi-scale bending, buckling and vibration analyses of carbon fiber/carbon nanotube-reinforced polymer nanocomposite plates with various shapes. Physica E 2017;93:17–25.

[11] Mehri M, Asadi H, Kouchakzadeh MA. Computationally efficient model for flow-induced instability of CNT reinforced functionally graded truncated conical curved panels subjected to axial compression. Comput Methods Appl Mech Eng 2017;318:957–80.

[12] Duc ND, Van Thu P. Nonlinear stability analysis of imperfect three-phase polymer

composite plates in thermal environments. Compos Struct 2014;109:130–8.
[13] Wu H, Kitipornchai S, Yang J. Thermal buckling and postbuckling of functionally graded graphene nanocomposite plates. Mater Des 2017;132:430–41.
[14] Conibeer G. Third-generation photovoltaics. Mater Today 2007;10:42–50.
[15] Miles RW, Zoppi G, Forbes I. Inorganic photovoltaic cells. Mater Today 2007;10:20–7.
[16] REN21. Renewables 2015-Global status report. vol. 4. 2015.
[17] Tao Y, Yang C, Qin J, Tang CW, VanSlyke SA, Baldo MA, et al. Organic host materials for phosphorescent organic light-emitting diodes. Chem Soc Rev 2011;40:2943.
[18] Stratakis E, Kymakis E. Nanoparticle-based plasmonic organic photovoltaic devices. Mater Today 2013;16:133–46.
[19] Linic S, Christopher P, Ingram DB. Plasmonic-metal nanostructures for efficient conversion of solar to chemical energy. Nat Mater 2011;10:911–21.
[20] Kim K, Carroll DL. Roles of Au and Ag nanoparticles in efficiency enhancement of poly(3-octylthiophene)/C_{60} bulk heterojunction photovoltaic devices. Appl Phys Lett 2005;87:203113.
[21] Rand BP, Peumans P, Forrest SR. Long-range absorption enhancement in organic tandem thin-film solar cells containing silver nanoclusters. J Appl Phys 2004;96:7519–26.
[22] Morfa AJ, Rowlen KL, Reilly TH, Romero MJ, Van De Lagemaat J. Plasmon-enhanced solar energy conversion in organic bulk heterojunction photovoltaics. Appl Phys Lett 2008;92:4–7.
[23] Vanin GA, Duc ND. Theory of spherofibrous composite.⁎ 1. input relationships: hypotheses and models 1996;32:197–207.
[24] Keleshteri MM, Asadi H, Wang Q. Large amplitude vibration of FG-CNT reinforced composite annular plates with integrated piezoelectric layers on elastic foundation. Thin-Walled Struct 2017;120:203–14.
[25] Keleshteri MM, Asadi H, Wang Q. Postbuckling analysis of smart FG-CNTRC annular sector plates with surface-bonded piezoelectric layers using generalized differential quadrature method. Comput Methods Appl Mech Eng 2017;325:689–710.
[26] Shackelford JF, Alexander W. Materials science and engineering handbook. CRC Press LLC; 2001.
[27] Duc ND. Mechanics of nano-composite materials. J Sci: Math – Phys, Vietnam National University, Hanoi 2003;19(4):13–8.
[28] Duc ND, Tung HV, Hang DT. A method for determining the bulk modulus of composite material with sphere pad seeds. J Sci, Math – Phys, Vietnam National University, Hanoi 2006;22(2):17–20.
[29] Asadi H, Akbarzadeh AH, Wang Q. Nonlinear thermo-inertial instability of functionally graded shape memory alloy sandwich plates. Compos Struct 2015;120:496–508.
[30] Asadi H, Akbarzadeh AH, Chen ZT, Aghdam MM. Enhanced thermal stability of functionally graded sandwich cylindrical shells by shape memory alloys. Smart Mater Struct 2015;24(4):045022.
[31] Brush DD, Almroth BO. Buckling of bars, plates and shells. Mc. Graw-Hill; 1975.
[32] Reddy JN. Mechanics of laminated composite plates and shells: theory and analysis. Boca Raton: CRC Press; 2004.
[33] Duc ND. Nonlinear static and dynamic stability of functionally graded plates and shells. Hanoi, Vietnam: Vietnam National University Press; 2014.
[34] Park SY, Jeong WI, Kim DG, Kim JK, Lim DC, Kim JH, et al. Large-area organic solar cells with metal subelectrode on indium tin oxide anode. Appl. Phys. Lett. 2010;96(17):173301.